Transcriptomics and Co-expression Network Profiling of Effects of Levamisole Hydrochloride on *Bursaphelenchus Xylophilus*

Jie Chen
Northeast Forestry University
Buyong Wang
Heze University
Xin Hao
Northeast Forestry University
Jialiang Pan
State Forestry Administration
Ling Ma (975589952@qq.com)
Northeast Forestry University

Research article

Keywords: Bursaphelenchus xylophilus, Levamisole hydrochloride, transcriptome, STEM, Spearman

Posted Date: January 11th, 2021

DOI: https://doi.org/10.21203/rs.3.rs-142801/v1

Abstract

Background: *Bursaphelenchus xylophilus* is one of the most dangerous forest pathogens in the world, resulting in the devastating death of pine forests and causing great economic losses and forest ecological damage to the affected areas. To explore the effect of levamisole hydrochloride (LH) as an effective control agent on nematode.

Results: The results indicated that 2.5 mg/mL and 3.5 mg/mL LH had the toxicological effect on *B. xylophilus*, and the mortality increased significantly with the increase of concentration ($P<0.05$). We found and studied Sodium / Chloride and other ion genes belonging nervous system were up-regulated and the ion signal transmitted to the muscle protein and cause disorders, producing body-wall muscle twitchin, paralysis, and ultimately death. In the other hand, 2 Senecionine N-oxygenase and 2 Alcohol dehydrogenase as the central genes in drug metabolism-cytochrome P450 (ko00982) and metabolism of xenobiotics by cytochrome P450 (ko00980), and 8 highly related genes including Cuticle collagen, Cystathionine beta-synthase, Endochitinase, Pyruvate dehydrogenase E1 component subunit beta, Aldehyde dehydrogenase, Lipase, Zinc metalloproteinase. Their expressions up-regulation significantly at low concentrations and were significantly related to the resistance of *B. xylophilus* to LH.

Conclusion: This study has shown that *B. xylophilus* gene family expansions occurred in xenobiotic detoxification pathways through the degree of genes expression and potential horizontal correlated gene transfer with LH, and shed light on LH lethality and evolutionary mechanisms behind adaptations of *B. xylophilus* to the environment. These findings contribute in several ways to our understanding of *B. xylophilus* under LH and provide a basis for control of it.

Background

Pine wilt disease (PWD) caused by *Bursaphelenchus xylophilus* has caused serious damage to pine trees, resulting in significant economic and ecological loss[1, 2]. *B. xylophilus* is native to North America, where it does not cause mortality in endemic hosts, occurring sporadically[3, 4]. When it was exported to Japan, South Korea, and China in East Asia with diseased trees, it caused devastating damage to the local pine ecosystem[2, 5, 6].The problem of *B. xylophilus* caused widespread concern. Nematocide injection into tree trunks is one of the most widely used comprehensive control measures at present, but the effect is not ideal because of its hidden harm[7–9]. So far, there have been many reports about natural nematicidal phytochemicals from various genera. Avermectin injection is often used in South Korea to protect pine[10], but its high prices limit the feasibility of its widespread use. Chemical nematicidal agents, such as fosthiazate carbofuran[11, 12], are mostly broad-spectrum and non-specific. While controlling nematodes, they are also very easy to harm non-harrowing organisms, including natural enemy insects, such as *Scleroderma guani* Ichneumonidae. It is urgent to find specific, efficient, and cheap nematicidal agents.

Levamisole hydrochloride is a white crystalline powder with a broad-spectrum, highly effective and low toxic nematicide. It is effective against gastrointestinal nematodes in many animals[13], but harmless to mammalian hosts, and even has can improve immunity to individuals with low immunity[14]. It was first proposed that acted on the drug-resistant mutant of acetylcholine receptors in *Caenorhabditis elegans*[15]. Later, it was confirmed that LH selectively acted on nicotinic acetylcholine receptor (nAChRs) on the somatic muscle and nerve of *C. elegans*, resulting in contraction and spastic paralysis of nematode[16, 17].In addition, nAChRs was found in the non-excited tissues. Among them, the L-AChR is the target of nematocide agents, such as levamisole and pyrantel, which, by acting as potent agonists, produce body-wall muscle hypercontraction, paralysis, and ultimately death[18]. Recent studies have shown that in addition to neuroreceptors, it has been found that intestinal nAChRs, activated by levamisole in *Ascaris lumbricoides* can promote the uptake and digestion of intestinal contents of nematodes[19]. But the targets of plant-parasitic nematodes have not been studied.

There is an urgent need to address the specific, efficient, and inexpensive control of these problems caused by *B. xylophilus*. Little is known about *B. xylophilus* xenobiotic detoxification and immunity, and it is not clear what factors of LH metabolism. To explore the genetic basis of adaptation of *B. xylophilus* to LH, *t*he transcriptome data were compared with those of *B. xylophilus*[20]. We studied pathogenesis, xenobiotic detoxification pathways, and candidate detoxification genes were identified. We propose that *B. xylophilus* response to LH was varied and complex, which facilitated its survival in LH environment. This is the first time to study the effect of LH to *B. xylophilus* and to explore the response mechanism of it.

Results

Effects of LH on the activity of B. xylophilus

By toxicity test, the higher the concentration of LH, the higher the mortality of *B. xylophilus* with significant difference ($P < 0.05$) (Fig. 1). The highest mortality rate of LH (3.5 mg/mL) was 55% (Additional file 1).

RNA sequencing and quality evaluation.

After removing rRNA and low-quality readings, 515,955,240 high-quality clean readings were obtained from nine samples (Table 1). In all data, the mass value ≥ 30 base ratios were more than 94.13%, and the proportion of total readings located to the reference genome was between 68.15% and 75.28%. The conversion of the Counts to FPKM. Dendrogram clustering of the samples for each RNA sequencing showed a conservative comparison between samples. At the same time, the Pearson correlation value of repeated samples was significantly higher than that of inter-processing correlation (Fig. 2).

Table 1
Statistics analysis of RNA sequencing data

Sample	Clean Reads	Obtained Bases(G)	Q30 percentage(%)	GC percentage(%)	Mapped Reads
CK_1	60,660,788	8.96	93.73%	48.35%	41,337,842 (68.15%)
CK_2	56,835,218	8.39	94.13%	48.28%	39,293,205 (69.14%)
CK_3	56,991,226	8.35	94.34%	48.25%	39,641,735 (69.56%)
YD_1	59,089,760	8.77	96.02%	47.99%	44,261,105 (74.90%)
YD_2	61,068,882	9.08	95.92%	48.03%	45,971,711 (75.28%)
YD_3	68,908,552	10.23	95.96%	47.75%	51,360,037 (74.53%)
YG_1	47,374,798	6.98	96.36%	48.42%	33,924,629 (71.61%)
YG_2	48,427,104	7.17	96.23%	48.32%	35,122,307 (72.53%)
YG_3	56,598,912	8.38	96.33%	48.23%	40,694,487 (71.90%)

Note: Obtained bases: Obtained Reads: obtained Reads multiplied by sequence length. Q30 (%): calculate the percentage of bases with Phred values greater than 30 to the total bases. GC (%): calculate the percentage of the total number of bases G and C to the total number of bases.

Differentially Expressed Genes identification in B. xylophilus with the different concentrations of LH

Totally 8,279, 14,056, 10,200, 9,870, 4,554 and 5,515 genes were annotated in GO, Nr, Swissprot, KOG, COG and KEGG. By analyzing the transcriptome data of B. xylophilus with different concentrations of LH, a total of 487 DEGs were identified. Among them, 336, 384, 6 genes were significantly in Group CK_vs_Group YD, Group CK_vs_Group YG, and Group YD_vs_Group YG (Table 2).

Table 2
Comparisons of numbers of DEGs at different times

DEG set	All DEG	Up-regulated	Down-regulated
Group CK_vs_Group YD	336	141	195
Group CK_vs_Group YG	384	210	174
Group YD_vs_Group YG	6	5	1

GO enrichment showed that the DEGs were distributed in 45 categories of biological process, cell composition, and molecular function. In the different groups, the DEGs in biological processes were mainly related to cellular process, multicellular organismal process, metabolic process, biological regulation, response to stimulus; cell composition, cell, organelle, membrane; molecular function, catalytic activity, binding, transporter activity (Additional file 3). 7 GOs were significantly enriched in 3 subsets and 32 GOs were significantly enriched in 3 subsets (Fig. 3A). To evaluate the biological and functional significance of DEGs, pathway enrichment analysis was carried out using the KEGG database. A total of 16 pathways was annotated in the KEGG database. The main KEGG pathways included several drug metabolism related pathways, such as drug metabolism - cytochrome P450 (ko00982), metabolism of xenobiotics by cytochrome P450 (ko00980) (Additional file 2). These genes groups include four Senecionine N-oxygenase (FMO) (BUX.gene.s00600.44, BUX.gene.s00713.800, BUX.gene.s01092.255, BUX.gene.s01167.44), 2UDP-glucuronosyl transferase (UGT) (BUX.gene.s01147.195,BUX.gene.s00983.18),2 Glutathione S-transferase (GST) (BUX.gene.s00647.119,BUX.gene.s01518.76), 3 Alcohol dehydrogenase (ADH) (BUX.gene.s01063.85, BUX.gene.s01147.198, BUX.gene.s01281.195), 1Juvenile hormone epoxide hydrolase (BUX.gene.s00298.34) (Fig. 3B)(Additional file 4).

Predictive functional analysis of the highly expressed genes for different types of profile

487 DGEs were obtained from nine groups (control, 2.5 mg/mL and 3.5 mg/mL). According to the different trends of genes expression under different conditions, a set of unique model expression trends (similarity > 0.7) were identified. The trend of FPKM of different concentrations of DGEs was analyzed by STEM software, and eight differential mRNA expression trends were calculated by using the significant expression of gene array, of which three profiles were drawn in the color part (profile 1,6 and 7 DEGs $p < 0.01$) (Fig. 4A). The significant trend of Profile1 (including 172 DEGs) showed that the expression level in DEPC-H2O (CK) was significantly higher than that in 2.5 mg/mL LH (YD). However, there was no significant change from YD group to 3.5 mg / ml LH (YG) group (Fig. 4B). The significant trend of profile 6 and profile 7 containing 161and 58 DEGs, from profile 6 and 7 showed a sharp up-regulation from CK group to YD group, and there was no significant change from YD group to YG group in profile 6 (Fig. 4C), but the DEGs expression level increased significantly in profile 7 (Fig. 4D).

Functional analysis of genes in different Profiles in order to understand the function related to drug resistance of B. xylophilus. 77 DEGs have been annotated and enriched to GO terms in profiles 6 ($P < 0.05$), most of them were enriched with “macromolecule metabolic process”, “actin filament fragmentation”, “actin nucleation” as biological processes. Most of them were enriched with “striated muscle dense body” as cellular components, and “oxidoreductase activity”, “peptidase activity” as molecular function (Fig. 5C). In profiles 6, “Glycolysis / Gluconeogenesis” (ko00010), “Lysosome” (ko04142), “Retinol metabolism”(ko00830), “Drug metabolism - cytochrome P450”(ko00982), “Degradation of aromatic compounds” (ko01220) significant enrichment (Fig. 5B). Meanwhile,43 DEGs have been annotated in KEGG data, including “Fatty acid degradation” (ko00071), “Metabolism of xenobiotics by cytochrome P450” (ko00980) and so on (Fig. 5A).

24 DEGs have been annotated and enriched to GO terms (belonging to biological process, cellular component, molecular function, $P < 0.05$), most of them were enriched with “monooxygenase activity” as molecular functions. Most of them were enriched with “peroxisome” be enriched, intracellular organelle part” as cellular components, and “long-chain fatty acid metabolic process”, “cellular nitrogen compound metabolic process”, “organic cyclic compound biosynthetic process”, “multicellular organism reproduction”, “peroxisome” as biological process (Fig. 6C). “Drug metabolism - cytochrome P450 (ko00982)”,” Phagosome (ko04145)”,” Peroxisome (ko04146)” were significant enrichment ($p < 0.05$) in Profiles 7 (Fig. 6B). “Glutathione metabolism”, “Metabolism of xenobiotics by cytochrome P450” and other signal pathways appeared in Profiles7 (Fig. 6A).

Construction and analysis of the co-expression network

According to the sequencing data, DEGs were selected as the centre genes in the xenobiotic detoxification pathways, including drug metabolism-cytochromeP450 (ko00982) and metabolism of xenobiotics by cytochrome P450 (ko00980). FMO (BUX.gene.s00600.44, BUX.gene.s00713.800), ADH (BUX.gene.s01281.195, BUX.gene.s01147.198) (Table S4) as the central gene were used to constructed a co-expression network, associating with a total of 54 genes ($p < 0.05$) (Additional file 5). There was a significant correlation between the two central genes of BUX.gene.s01147.198 and BUX.gene.s00713.800. Except for the unidentified proteins, a total of 8 DEGs were significantly associated with central genes (linking two or more central genes) (Fig. 7) (Additional file 7). qRT-PCR analysis confirmed that the expression trend of Endochitinase (BUX.gene.s00609.89), Cuticle collagen (BUX.gene.s00540.1). Lipase (BUX.gene.s01661.12), Pyruvate dehydrogenase E1 component subunit beta (BUX.gene.s01066.55), Aldehyde dehydrogenase (ALDH) (BUX.gene.s01144.247)were "up-up-basically stable", which were consistent with those obtained from the RNA sequencing analysis (Fig. 9).

GST (BUX.gene.s01518.76),FMO (BUX.gene.s00600.44) were used as the central gene to construct a co-expression network (Additional file 4). The correlation coefficient between the central gene and other genes was visualized by Profiles7 (Additional file 6). Except for the unidentified protein, FMO was significantly correlated with 4 DEGs, including Cuticle collagen (BUX.gene.s00252.94), Zinc metalloproteinase (BUX.gene.s00579.211), Cystathionine beta-synthase (BUX.gene.s00083.35) (Fig. 8)

(Additional file 8). And the expression trends of these genes were always up-regulated, consistent with RNA sequencing analysis (Fig. 9).

Discussion

B. xylophilus is highly destructive to pines. Until now, there is a lack of effective prevention and control of it. So, genes in the xenobiotic metabolism were very important to speculate the target for the control of *B. xylophilus*[21]. In eukaryotes, genes in the xenobiotic metabolism can remove drugs from cells, resulting in a decrease in intracellular drug concentration, contributing for drug resistance[22]. Several studies have already shown the multilayer detoxification of *B. xylophilus* against plant defences, which involves the detoxification and xenobiotic metabolic pathways of the nematode. Even there is a study on the effect of emamectin benzoate in *B. xylophilus* with the same approach. So, it is necessary to study the function of xenobiotic metabolism in order to provide theoretical basis for the development of LH control methods and targets. LH is a broad-spectrum, high-efficiency, and low-toxic nematicide, which has a good killing effect on chicken, sheep, and human gastrointestinal nematodes[13]. The effect of LH, xenobiotic detoxification and pathogenic mechanism of *B. xylophilus* has important value and provides a theoretical basis for prevention *B. xylophilus*.

Nine RNA libraries directly reflected the effect of LH on the genetic activity of *B. xylophilus*. Among the 32 common Gene Ontology (Fig. 3A), antioxidant activity, catalytic activity, detoxification, immune system process, molecular transducer activity, synapse, synapse part, transporter activity, signal transducer activity showed that LH treatment had a significant effect on the neural transmission and immune system of *B. xylophilus*[23]. The single-organism process was only in the group of YDvsYG, includes a 3'5'-cyclic nucleotide phosphodiesterase and 3 Cuticle collagen, which were significantly up-regulated from low concentration to high concentration. The Cuticle collagen, an extracellular collagen matrix that surrounds *C. elegans*, is the first barrier against environmental damage, protecting nematodes from pathogens, dryness, and other stress[24–26]. The up-regulation of the high concentration of Cuticle collagen indicated that the integument of *B. xylophilus* thickened, the resistance of nematodes was enhanced. Xenobiotic detoxification pathways with drug metabolism - cytochrome P450 (ko00982) and metabolism of xenobiotics by cytochrome P450 (ko00980) were found, including most of the up-regulation FMO, UDT, GST, ADH and a Juvenile hormone epoxide hydrolase down-regulations (Fig. 3B) (Additional file 4). Compared with *C. elegans*, *B. xylophilus* has specific gene up-regulation in FMOs branch (FMO-5, FMO-10), which has a function similar to cytochrome P450 and adds molecular oxygen to insoluble xenobiotic organisms. Many insects and microorganisms can metabolize chemicals into less toxic or more soluble compounds. They use cytochrome P450 or FMO to oxidize it to alcohols, then ADHs to oxidize alcohols to aldehydes/ketones[22], and finally ALDHs to oxidize these products to acids for subsequent metabolism or transport. ADH is one of the key genes regulating the dynamic behavior of *B. xylophilus*[27]. P450, UGT, glutathione -S transferase, Redox, dehydrogenase, and reductase of *C. elegans* under five different Benzimidazole drugs increased. UGT are enzymes that are glucuronidated the substrates include drugs, environmental toxins, and endogenous compounds. And the products are water-soluble and readily excreted[28]. UGT inhibitors resulted in a decrease of metabolite production in

nematode and the decrease of drug resistance[29]. UGT inhibitor increased the sensitivity of wild type *H. contortus* to naphtalophos (anthelmintic)[30]. GST can catalyze the binding of glutathione with electrophilic groups of chemical substances, and eventually form mercapturic acid to be excreted in vitro[31]. And 3 GST and P450 were upregulated contributed to mitigating tetrabromobisphenol A-induced toxicity on the *C. elegans*[32]. Thus, based on the results and previous studies, UDT, GST, FMO, ADH, Juvenile hormone epoxide hydrolase were considered as one of the main factors of *B. xylophilus* detoxification ability.

Sets of profiles were predefined which were expected in the process of genetic changes. These sets of profiles cover all of the possible gene expression changes, and each represents a single drug concentration expression pattern. Profile significance levels were determined by gene enrichment, and significant profiles indicate the most common functions of co-expressed genes, with the main biological character[33–35]. Xenobiotic detoxification pathways, such as Glycolysis/ Gluconeogenesis, Glutathione metabolism, Metabolism of xenobiotics by cytochrome P450, Drug metabolism-cytochrome P450 were significant enrichment. Also, Lysosome, Phagosome, Peroxisome, and other immune-related pathways were significantly enriched (Fig. 5B Fig. 6B), indicating that the innate immune defense of *B. xylophilus* increased, such as Lysosome, Cysteine proteinase, and transthyretin-like proteins[36]. On the other hand, it has been reported that LH has the function of enhancing immune response by enhancing phagocytosis[37–39]. LH is a typical deworming drug that activates nematode nAChR, which acts as a powerful agonist in muscle contraction and movement and is a key target[36, 40]. NAChR transfers the ion signal to disorganized muscle protein through Sodium/Chloride and causes gene up-regulation, produce body-wall muscle twitchin, paralysis, and ultimately death in *B. xylophilus* (Additional file 9). This is one of the direct causes of the death of *B. xylophilus*, but how LH acts on the nervous system signal transduction process of *B. xylophilus* awaits further exploration (Fig. 10) (Additional file 10 A).

Genes in the same biological pathway are more likely to be co-expressed to synchronize an array of biochemical reactions[41, 42]. We studied the connectivity patterns of drug metabolism-cytochromeP450 (ko00982) and metabolism of xenobiotics by cytochrome P450 (ko00980) pathways in profile1and profile 6 gene expression data. In Profiles 6, we observed that 54 genes were associated with the correction of Pearson, that is, the corresponding P-value was < 0.05. FMO (BUX. Gene. S00600.44, BUX. Gene. S00713.800) and ADH (BUX. gene. S01281.195, BUX. gene. S01147.198) were significant correlation in the center gene (Fig. 7), which were highly consistent with the previous conjecture that its play important role in xenobiotics metabolism. Among them, highly correlated Cuticle collagen(BUX.gene.s 00540.1)[25]; Lipase (BUX.gene.s 01661.12)[37]; ALDH (BUX.gene.s01144.247)[22] all produced proteins related to nematode immunity. Pyruvate dehydrogenase E1 component subunit beta (BUX.gene.s01066.55) is highly related to the TCA cycle and mitochondrial energy metabolism, providing energy for the growth and development of nematodes[38, 39, 43]. We speculate that pyruvate dehydrogenase was significantly up-regulated because of aldehyde and ketone oxidase oxidated intermediate (disulfide). In profiles1, we observed that cuticle collagen (BUX.gene.s00252.94)[25]; Zinc metalloproteinase (BUX.gene.s00579.211) as zinc matrix metalloproteinases can improve the resistance to high temperature and bacteria in *C. elegans*[44]; Cystathionine beta-synthase (BUX.gene.s00083.35)

provides cysteine, which is important for the formation of the stratum corneum in *C. elegans*. As well as, it produces neuromodulator and smooth muscle relaxant hydrogen sulfide in muscle and subcutaneous tissue[45–47].

In conclusion, from the transcriptomes of *B. xylophilus* treated with 2.5 mg /mL,3.5 mg/mL LH, and DEPC-H_2O, with STEM and Spearman correlation, pathogenesis, xenobiotic detoxification pathways, and candidate detoxification genes were identified. We propose that *B. xylophilus* response to LH was varied and complex which facilitated its survival in LH environment (Fig. 10) (Additional file 10 B). However, this is the first time to study the effect of LH on *B. xylophilus* and to explore the resistance mechanism of *B. xylophilus* and these findings contribute in several ways to our understanding of *B. xylophilus* under LH. Lays the groundwork for future research into LH could also be conducted to determine the effectiveness of control of *B. xylophilus*.

Materials And Methods

Sample B. xylophilus

B. xylophilus were cultured on the solid medium of *Botrytis cinerea* from *Pinus massoniana* .provided by the Forest Pest Biology Laboratory of Northeast Forestry University at 25 ℃ in the dark. It was collected by the improved Baermann funnel method. And, the nematode were washed with double distilled water, removing by 4000 rpm in 5 min. There were about 10000 nematodes in 1 ml DEPC-H_2O. The 2.5 mg/mL and 3.5 mg/mL LH (99% purity, Shanghai Aladdin Company) were prepared with DEPC-H_2O. 1 ml *B. xylophilus* was added to the final concentrations YD group (2.5 mg/mL), the YG group (3.5 mg/mL), and the CK group (DEPC-H_2O) respectively, and mixed well. After 12 hours, the number of nematodes was counted by the dilution concentration method on the 24-well plate, under the anatomical microscope. The phenotype of the nematodes was observed, and the mortality rate was calculated (the body was stiff and the nematodes that did not move when touching the needle were dead). The biologicalexperiment was repeated 6 times. Nematodes were washed with double distilled water and DEPC-H_2O, removing by 4000 rpm in 5 min. Then nematodes were frozen in liquid nitrogen and stored at -80℃ for RNA extraction. The One-way ANOVA (Duncan's) of the data was performed using IBM SPSS Statistics 19.

$$Mortality\ \ Rate(\%) = \frac{Dead\ \ Number}{Total\ \ Number} \times 100,$$

RNA extraction, library construction, RNA sequencing and assembly

From 9 samples, TRIzol reagent (Invitrogen, USA) was used to extract total RNA. RNA degradation and contamination was monitored on 1% agarose gels. RNA purity was checked using the NanoPhotometer spectrophotometer (IMPLEN, CA, USA). RNA concentration was measured using Qubit RNA Assay Kit in

Qubit 2.0 Flurometer (Life Technologies, CA, USA). RNA integrity was assessed using the RNA Nano 6000 Assay Kit of the Agilent Bioanalyzer 2100 system (Agilent Technologies, CA, USA).

A total amount of 1 μg RNA per sample was used as input material for the RNA sample preparations. Sequencing libraries were generated using NEBNext UltraTM RNA Library Prep Kit for Illumina (NEB, USA) following manufacturer's recommendations and index codes were added to attribute sequences to each sample. Briefly, mRNA was purified from total RNA using poly-T oligo-attached magnetic beads. Fragmentation was carried out using divalent cations under elevated temperature in NEBNext First Strand Synthesis Reaction Buffer(5X). First strand cDNA was synthesized using random hexamer primer and M-MuLV Reverse Transcriptase. Second strand cDNA synthesis was subsequently performed using DNA Polymerase I and RNase H. Remaining overhangs were converted into blunt ends via exonuclease/polymerase activities. After adenylation of 3' ends of DNA fragments, NEBNext Adaptor with hairpin loop structure were ligated to prepare for hybridization. In order to select cDNA fragments of preferentially 200–250 bp in length, the library fragments were purified with AMPure XP system (Beckman Coulter, Beverly, USA). Then 3 μl USER Enzyme (NEB, USA) was used with size-selected, adaptor-ligated cDNA at 37 °C for 15 min followed by 5 min at 95 °C before PCR. Then PCR was performed with Phusion High-Fidelity DNA polymerase, Universal PCR primers and Index (X) Primer. At last, PCR products were purified (AMPure XP system) and library quality was assessed on the Agilent Bioanalyzer 2100 system The clustering of the index-coded samples was performed on a cBot Cluster Generation System using TruSeq PE Cluster Kit v4-cBot-HS (Illumia) according to the manufacturer's instructions. After cluster generation, the library preparations were sequenced on an Illumina Hiseq 2500 platform and paired-end reads were generated by BIOMARKER Biotechnology Co., Ltd. (Beijing, China). Raw data (raw reads) of fastq format were firstly processed through in-house perl scripts. In this step, clean data(clean reads) were obtained by removing reads containing adapter, reads containing ploy-N and low quality reads from raw data. At the same time, Q20, Q30, GC-content and sequence duplication level of the clean data were calculated. All the downstream analyses were based on clean data with high quality.

The adaptor sequences and low-quality sequence reads were removed from the data sets. Raw sequences were transformed into clean reads after data processing. These clean reads were then mapped to the reference genome sequence. Only reads with a perfect match or one mismatch were further analyzed and annotated based on the reference genome. Then use TopHat2 (version 2.0.3.12)[48] to map the clean readings of each sample to the reference genome[20]. Based on the Cufflinktware, the FPKM method quantified the gene expression level by comparing the location information on the genome[49].

Identification of differentially expressed genes (DEGs), Sequencing Data Analysis

The DESeq2 package (https://bioconductor.org/)[23] was used to identify DEGs across groups with fold changes ≥ 2and a false discovery rate (FDR) < 0.05. Basic annotation of genes includes NCBI non-

redundant protein (Nr) database, Kyoto Encyclopedia of Genes and Genomes (KEGG) pathway annotation, Clusters of orthologous groups of proteins (COG) functional annotation, Swiss-Prot protein database, and Gene Ontology (GO) annotation. DEGs were had to enrichment analysis by using the ClusterProfiler package (https://bioconductor.org/).

Trend analysis of DEGs

The differential gene expression was was calculated and normalized to FPKM. To evaluate the gene expression pattern of nematode under three different concentrations, DEGs were assigned to 8 different types of profiles by Short Time-series Expression Miner software (STEM)[50]. The maximum Unit Change in model profiles between points was 1 and the maximum output profile number was 20. The correlation coefficient between the gene expression pattern and the most similar trend > 0.7 was classified into the same model. Significant profiles were determined and the threshold of significance wa**s** considered as $p < 0.05$. Then the significant profiles were subjected to GO term enrichment and KEGG enrichment to research functions.

Construction of the co-expression network of the significant profiles-Spearman's rank correlation

In profiles, DEGs expression data set matrix calculated the Spearman correlation coefficient (rs) between the central gene and the other gene, and corrected (p) by cor.test package (R code). Removing the influence of gene itself and gene quantity[41], the genes with significant connection ($p < 0.05$) were selected to construct the expression-related network. The networks were visualized using Cytoscape_3.7.1.[51].

$$r_s = \frac{6\sum_{i=1}^{n} d_i^2}{n(n^2-1)},$$

d_i = the difference between the ranks of the i^{th} observations of the two variables. n = the number of pairs of values[41].

Validation of gene expression by qRT-PCR

Twelve DEGs were selected for qRT-PCR analysis. Primer 6.0 software was used to design the primers and completed by Sangon Biotech (Shanghai, China) (Additional file 9). Bx28S and Actin gene were selected as the housekeeping gene[52]. Agilent Technologies Mx3000P was used for real-time PCR detection, and qPCR was performed following the protocol provided by the TaKaRa One-Step RT-PCR Kit (Baori medical technology (Beijing) co., LTD, Beijing, China) and compared to using the threshold cycle ($-\Delta\Delta Ct$) method of gene expression.

Declarations

Ethics approval

This article does not contain any studies with human participants or animals performed by any of the authors.

Authors' contributions

Y. W. and L. M. designed the work; J. P., and X.H. performed the experiments; Y. W. and J. C. analyzed the data and wrote the paper.

Funding

This work was supported by grants from the Shandong Provincial Natural Science Foundation, grant number: ZR2019BC098 and the Fundamental Research Funds for the Central Universities, grant number:2572019CP01. The funders had a key role in the data analysis and interpretation of data.

Consent for publication

Not applicable.

Competing interest

The authors declared that they have no conflicts of interest to this work.

Acknowledgements

We are grateful to the Sangon Biotech (Shanghai, China) and BIOMARKER Biotechnology Co., Ltd. (Beijing, China) for technical and equipment assistance.

Consent for publication

The authors declared that they agree to publish this work.

Conflicts of Interest

The authors declared that they have no conflicts of interest in this work.

Availability of data and materials

All analyses tools used in the study are publicly available. NCBI non-redundant protein (Nr) database: http://www.ncbi.nlm.nih.gov; COG functional annotation: http://www.ncbi.nlm.nih.gov/COG; Swiss-Prot protein database: http://www.expasy.ch/sprot; KEGG Database: https://www.kegg.jp/; KEGG PATHWAY Database: https://www.kegg.jp/kegg/pathway; Gene Ontology Database: http://geneontology.org/; The DESeq2 and ClusterProfiler package are from R (https://bioconductor.org/), and the cor.test package is from R (http://r-project.org). All data generated or analyzed during this study are included in this published article and its supplementary information files.

References

1. Vicente C, Espada M, Vieira P, Mota M. Pine Wilt Disease: a threat to European forestry (vol 133, pg 89, 2012). Eur J Plant Pathol. 2012;133:497.
2. Zhao L, Sun J. Pinewood Nematode *Bursaphelenchus xylophilus* (Steiner and Buhrer) Nickle. Springer Singapore; 2017.
3. Kiyohara T, Bolla RI. Pathogenic variability among populations of the pinewood nematode, *Bursaphelenchus xylophilus*. For Sci. 1990;36:1061-1076.
4. Rutherford TA, Mamiya Y, Webster JM. Nematode-induced pine wilt disease: factors influencing its occurrence and distribution. For Ence. 1990;36:145-155.
5. Mamiya Y. History of pine wilt disease in Japan. J Nematol. 1988;20:219-226.
6. K. YC, H. BB, D. PJ, I. YS, H. CK. First finding of the pine wood nematode, *Bursaphelenchus xylophilus* (Steiner et Buhrer) Nickle and its insect vector in Korea. Res Reports For Res Inst. 1989;141-149.
7. James R, Tisserat N, Todd T. Prevention of Pine Wilt of Scots Pine (*Pinus sylvestris*) with Systemic Abamectin Injections. Arboric Urban For. 2006;32:195–201.
8. Sang ML, Dong SK, Sang GL, Park NC, Dong WL. Selection of Trunk Injection Pesticides for Preventive of Pine Wilt Disease, *Bursaphelenchus xylophilus* on Japanese Black Pine (*Pinus thunbergii*). Korean J Pestic Sci. 2009;13:267–274.
9. Yang B. Pine wood nematode disease. Bei Jing: China Forestry Publishing; 2003.
10. Kim J, Seo SM, Lee SG, Shin SC, Park IK. Nematicidal Activity of Plant Essential Oils and Components from Coriander (*Coriandrum sativum*), Oriental Sweetgum (*Liquidambar orientalis*), and Valerian (*Valeriana wallichii*) Essential Oils against Pine Wood Nematode (*Bursaphelenchus xylophilus*). J Agric Food Chem. 2008;56:7316–20.
11. Lai YL, Xiang MC, Liu SC, Li EW, Che YS, Liu XZ. A novel high-throughput nematicidal assay using embryo cells and larvae of *Caenorhabditis elegans*. Exp Parasitol. 2014;139:33-41.
12. Kang JS, Moon YS, Lee SH. Inhibition properties of three acetylcholinesterases of the pinewood nematode *Bursaphelenchus xylophilus* by organophosphates and carbamates. Pestic Biochem Physiol. 2012;104:157–62.
13. Zhang P, Wan Y, Zhang C, Zhao R, Sha J, Li Y, et al. Solubility and mixing thermodynamic properties of levamisole hydrochloride in twelve pure solvents at various temperatures. J Chem Thermodyn.

2019;139:105882.

14. Xuedan Y, Tongtong X, Yuanyuan L, Jun W. Effect of levamisole hydrochloride on the immune function in immunosuppressed mice. Chinese J Clin Pharmacol. 2019;550-552.
15. Lewis PA, Wu C Te, Levine J, Berg JH. The genetics of levamisole resistance in the nematode *Caenorhabditis elegans*. Genetics. 1980;95:905.
16. Culetto E, Baylis HA, Richmond JE, Jones AK, Fleming JT, Squire MD, et al. The *Caenorhabditis elegans* unc-63 Gene Encodes a Levamisole-sensitive Nicotinic Acetylcholine Receptor Subunit. J Biol Chem. 2004;279:42476–83.
17. Duguet TB, Charvet CL, Sean G. Forrester, et al. Recent Duplication and Functional Divergence in Parasitic Nematode Levamisole-Sensitive Acetylcholine Receptors. PLoS Negl Trop Dis. 2016;10.
18. Turani O, Hernando G, Corradi J, Bouzat C. Activation of *Caenorhabditis elegans* Levamisole-Sensitive and Mammalian Nicotinic Receptors by the Antiparasitic Bephenium. Mol Pharmacol. 2018;94:1270.
19. McHugh M, Williams P, Verma S, Powell-Coffman JA, Martin RJ. Cholinergic receptors on intestine cells of Ascaris suum and activation of nAChRs by levamisole. Int J Parasitol Drugs Drug Resist. 2020;13:38-50.
20. Kikuchi T, Cotton JA, Dalzell JJ, Hasegawa K, Kanzaki N, McVeigh P, et al. Genomic insights into the origin of parasitism in the emerging plant pathogen *Bursaphelenchus xylophilus*. PLoS Pathog. 2011;7:e1002219.
21. Li Y-L, Zheng C-Y, Liu K-C, Wu Y, Fan B, Han Z-M. Transformation of Multi-Antibiotic Resistant *Stenotrophomonas maltophilia* with GFP Gene to Enable Tracking its Survival on Pine Trees. Forests. 2019;10.
22. Zhang W, Yu H, Lv Y, Bushley KE, Wickham JD, Gao S, et al. Gene family expansion of pinewood nematode to detoxify its host defence chemicals. Mol Ecol. 2020;29:940–55.
23. Lu F, Guo K, Chen A, Chen S, Lin H, Zhou X. Transcriptomic profiling of effects of emamectin benzoate on the pine wood nematode *Bursaphelenchus xylophilus*. Pest Manag Sci. 2020;76:747-57..
24. Gravatonobre MJ, Vaz F, Filipe S, Chalmers R, Hodgkin J. The Invertebrate Lysozyme Effector ILYS-3 Is Systemically Activated in Response to Danger Signals and Confers Antimicrobial Protection in C. elegans. PLOS Pathog. 2016;12:e1005826.
25. Mesbahi H, Pho KB, Tench AJ, Leon GVL, MacNeil LT. Cuticle Collagen Expression Is Regulated in Response to Environmental Stimuli by the GATA Transcription Factor ELT-3 in *Caenorhabditis elegans*. Genetics. 2020;215:483–95.
26. Xiong H, Pears C, Woollard A. An enhanced *C. elegans* based platform for toxicity assessment. Sci Rep. 2017;7:9839.
27. Wang L, Zhang T, Pan Z, Lin L, Dong G, Wang M, et al. The alcohol dehydrogenase with a broad range of substrate specificity regulates vitality and reproduction of the plant-parasitic nematode *Bursaphelenchus xylophilus*. Parasitology. 2019;146:497–505.

28. Mackenzie PI, Gardner-Stephen DA, Miners JO. Comprehensive Toxicology. second edi. Netherlands: Elsevier Science; 2010.
29. Stasiuk SJ, MacNevin G, Workentine ML, Gray D, Gilleard JS. Similarities and differences in the biotransformation and transcriptomic responses of *Caenorhabditis elegans* and *Haemonchus contortus* to five different benzimidazole drugs. Int J Parasitol Drugs Drug Resist. 2019;11:13-29.
30. Kotze AC, Ruffell AP, Ingham AB. Phenobarbital Induction and Chemical Synergism Demonstrate the Role of UDP-Glucuronosyltransferases in Detoxification of Naphthalophos by *Haemonchus contortus* Larvae. Antimicrob Agents Chemother. 2014;58:7475–83.
31. Papadopoulos AI, Lazaridou E, Mauridou G, Touraki M. Glutathione S-transferase in the branchiopodArtemia salina. Mar Biol. 2004;144:295–301.
32. Lindblom TH, Dodd AK. Xenobiotic detoxification in the nematode *Caenorhabditis elegans*. J Exp Zool Part A Ecol Integr Physiol. 2006;305a:312.
33. Chen F, Zhu H-H, Zhou L-F, Li J, Zhao L-Y, Wu S-S, et al. Genes related to the very early stage of ConA-induced fulminant hepatitis: a gene-chip-based study in a mouse model. BMC Genomics. 2010;11:240.
34. Gracey AY, Fraser EJ, Li W, Fang Y, Taylor RR, Rogers J, et al. Coping with Cold: An Integrative, Multitissue Analysis of the Transcriptome of a Poikilothermic Vertebrate. PNAS. 2004;101:16970-16975.
35. Sun M, Li S, Zhang X, Xiang J, Li F. Isolation and transcriptome analysis of three subpopulations of shrimp hemocytes reveals the underlying mechanism of their immune functions. Dev Comp Immunol. 2020;108:103689.
36. Treitz C, Cassidy L, H Ckendorf A, Leippe M, Tholey A. Quantitative proteome analysis of *Caenorhabditis elegans* upon exposure to nematicidal Bacillus thuringiensis. J Proteomics. 2015;113:337-350.
37. O'Rourke D, Baban D, Demidova M, Mott R, Hodgkin J. Genomic clusters, putative pathogen recognition molecules, and antimicrobial genes are induced by infection of *C. elegans* with M. nematophilum. GENOME Res. 2006;16:1005–16.
38. Chapman KA, Ostrovsky J, Rao M, Dingley SD, Polyak E, Yudkoff M, et al. Propionyl-CoA carboxylase pcca-1 and pccb-1 gene deletions in *Caenorhabditis elegans* globally impair mitochondrial energy metabolism. J Inherit Metab Dis. 2018;41:157–68.
39. Schwab Marina A SSWO. Secondary mitochondrial dysfunction in propionic aciduria: a pathogenic role for endogenous mitochondrial toxins. Biochem J. 2006;398:107-112.
40. J. MR, P. RA. Mode of action of levamisole and pyrantel, anthelmintic resistance, E153 and Q57. Parasitology. 2007;134:1093–104.
41. Kumari S, Nie J, Chen HS, Ma H, Stewart R, Li X, et al. Evaluation of gene association methods for co-expression network construction and biological knowledge discovery. PLoS One. 2012;7:e50411.
42. Amitabh S, Jörg M, Huang CC, Tatiana O, Zhou X, Maksim K, et al. A disease module in the interactome explains disease heterogeneity, drug response and captures novel pathways and genes

in asthma. Hum Mol Genet. 2015;11:3005-3020.

43. Chen W, Komunieckl PR, Komunieckl R. Nematode pyruvate dehydrogenase kinases : role of the C-terminus in binding to the dihydrolipoyl transacetylase core of the pyruvate dehydrogenase complex. Biochem J. 1999;339:103–109.
44. Fischer M, Fitzenberger E, Kull R, Boll M. The zinc matrix metalloproteinase ZMP-2 increases survival of *Caenorhabditis elegans* through interference with lipoprotein absorption. Genes Nutr. 2014;9:414-424.
45. Ap P, Il J. The cuticle (The *C. elegans* Research Community, ed). Wormbook. 2007;1-15.
46. Kimura H. Hydrogen sulfide: its production, release and functions. Amino Acids. 2011;41:113–121.
47. Vozdek R, HnÍzda A, Krijt J, Kostrouchova M, Kozich V. Novel structural arrangement of nematode cystathionine β -synthases: characterization of Caenorhabditis elegans CBS-1. Biochem J. 2012;443:535–547.
48. Kim D, Pertea G, Trapnell C, Pimentel H, Kelley R. TopHat2: accurate alignment of transcriptomes in the presence of insertions, deletions and gene fusions. Genome Biol. 2013;14:R36.
49. Florea L, Song L, Salzberg SL. Thousands of exon skipping events differentiate among splicing patterns in sixteen human tissues. F1000res. 2013;2:188.
50. Ernst J, Bar-Joseph Z. STEM: a tool for the analysis of short time series gene expression data. BMC Bioinformatics. 2006;7:191.
51. Shannon P, Markiel A, Ozier O, Baliga NS, Wang JT, Ramage D, et al. Cytoscape: A software environment for integrated models of biomolecular interaction networks. GENOME Res. 2003;13:2498–504.
52. Wang B, Hao X, Xu J, Ma Y, Ma L. Transcriptome-Based Analysis Reveals a Crucial Role of BxGPCR17454 in Low Temperature Response of Pine Wood Nematode (*Bursaphelenchus xylophilus*). Int J Mol Sci. 2019;20:2898.

Figures

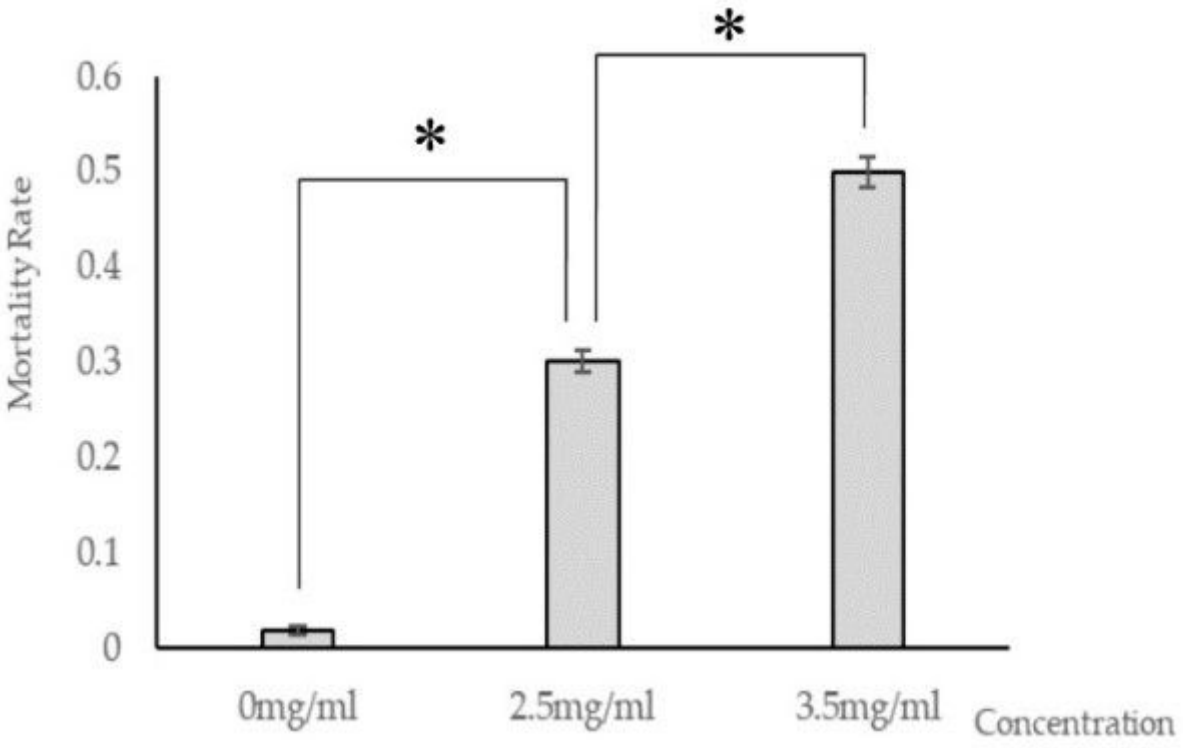

Figure 1

The mortality rate of B. xylophilus with different concentrations of LH. (*) It is a significant difference between the two groups ($p<0.05$).

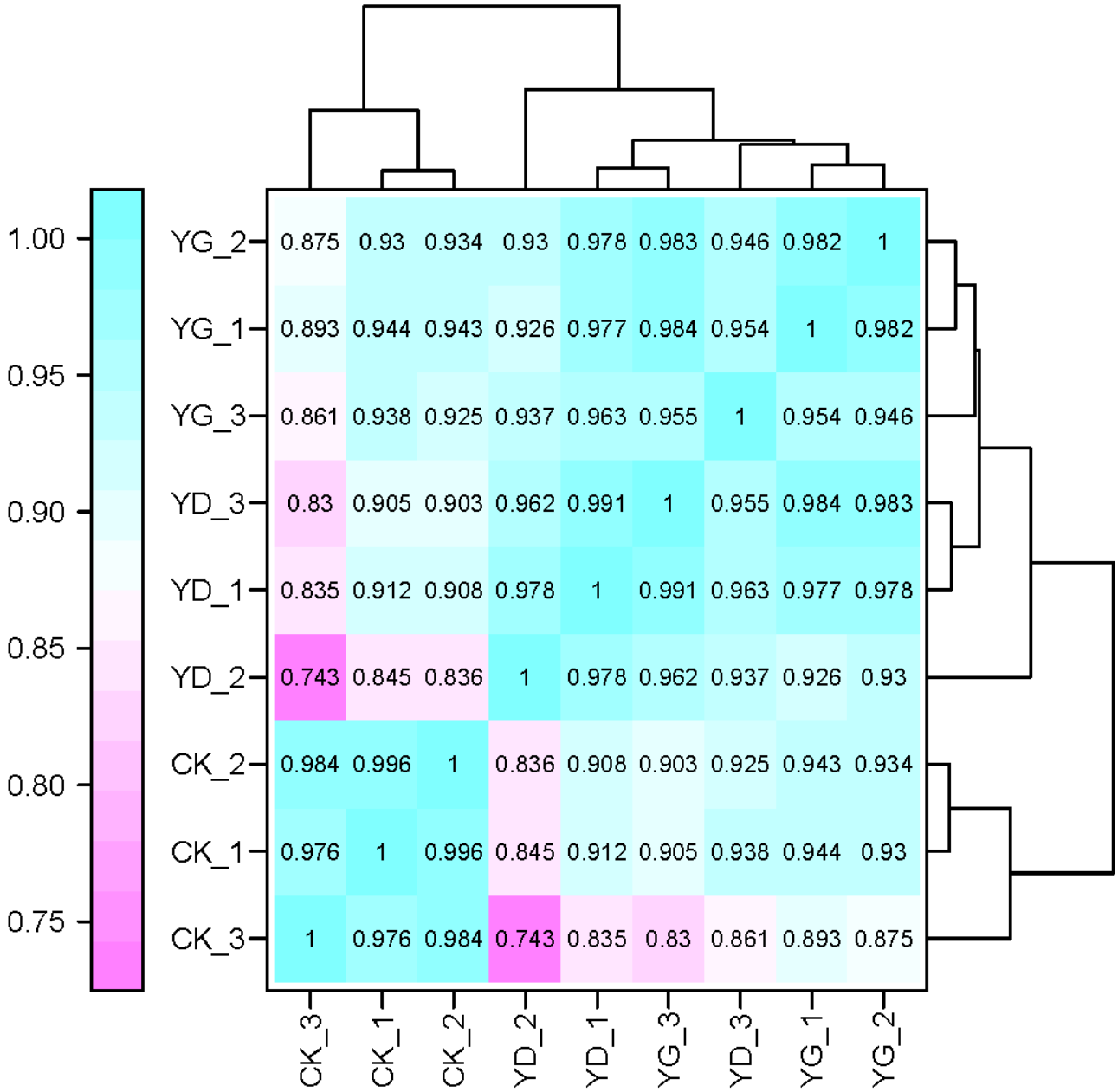

Figure 2

Correlation analysis of samples

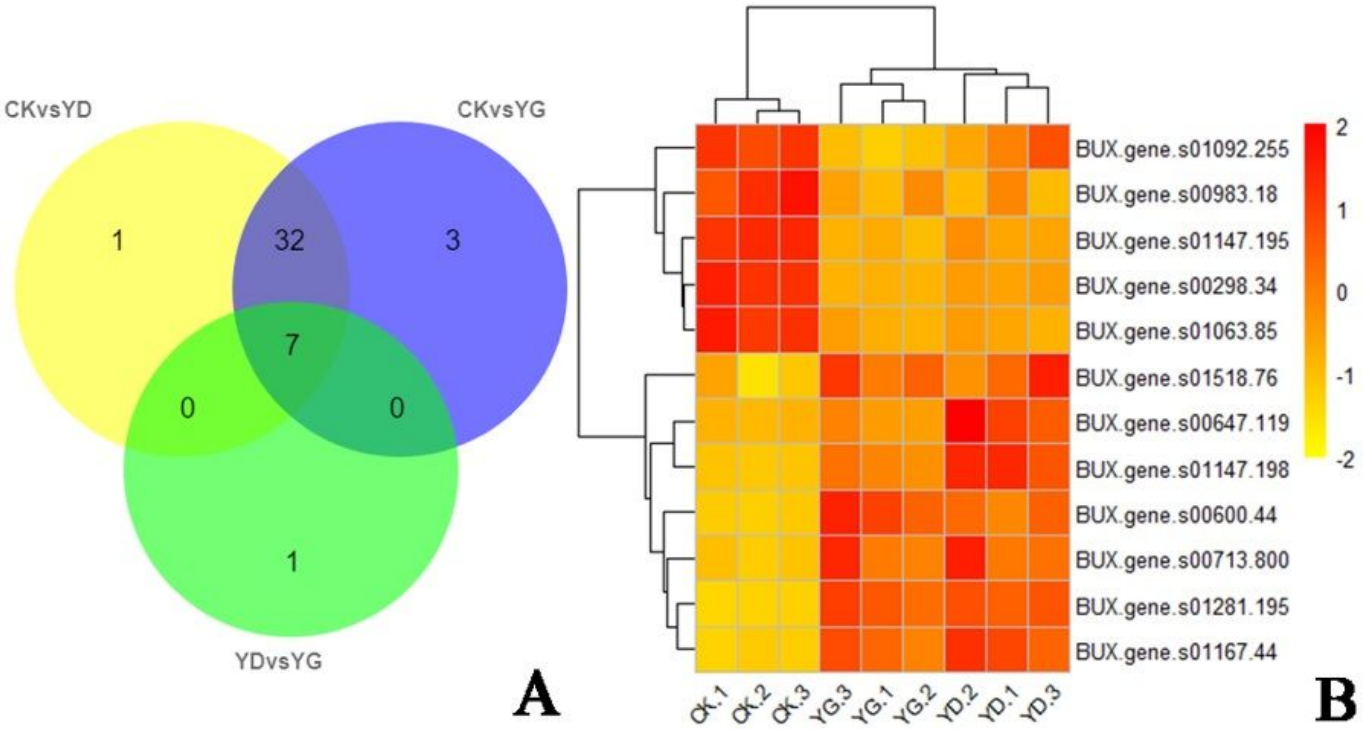

Figure 3

DEGs analysis. (A). Venn diagram of Gene Ontology (GO) categories of DEGs. (B). Heat map of the DEGs in drug metabolism and metabolism of xenobiotics. The expression counts were processed by log 2 and row normalization.

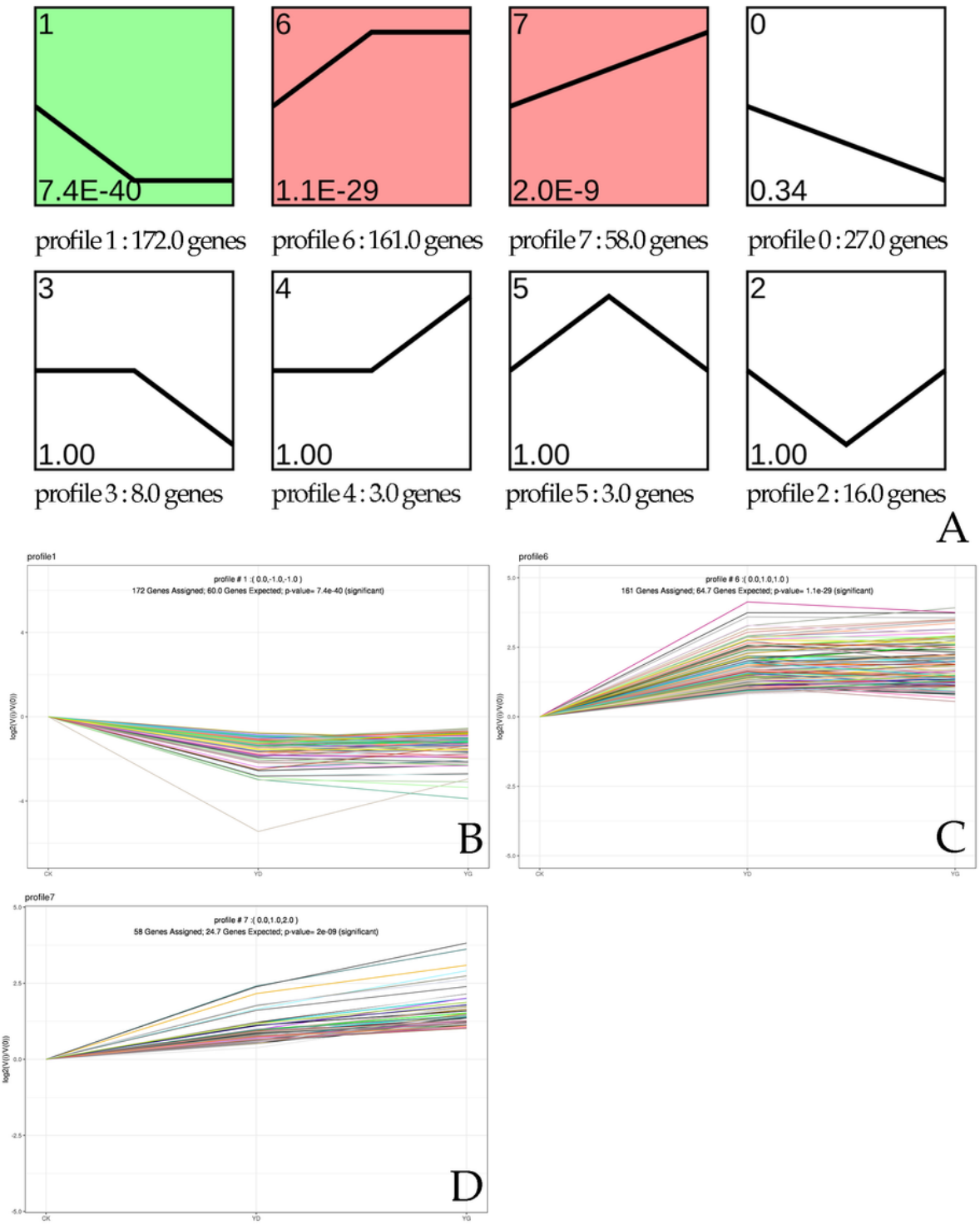

Figure 4

The expression patterns of 448 DEGs analyzed by model profile. (A). The expression patterns of 448 DEGs were analyzed and eight model profiles were used to summarize. Each box represents a model expression profile, the black line represented the expression tendency of all the genes. The inside number in the profile box is the model profile p-value; Three expression patterns of genes showed significant p-values ($p < 0.05$) (colored boxes); (B) Gene expression of profile No.1 in the context of significant the

different concentrations of LH; (C) Gene expression of profile No.6 in the context of significant the different concentrations of LH; (D) Gene expression of profile No.7 in the context of significant the different concentrations of LH. The horizontal axis represents the different concentrations of LH, and the vertical axis shows gene expression levels for the gene after Log normalized transformation.

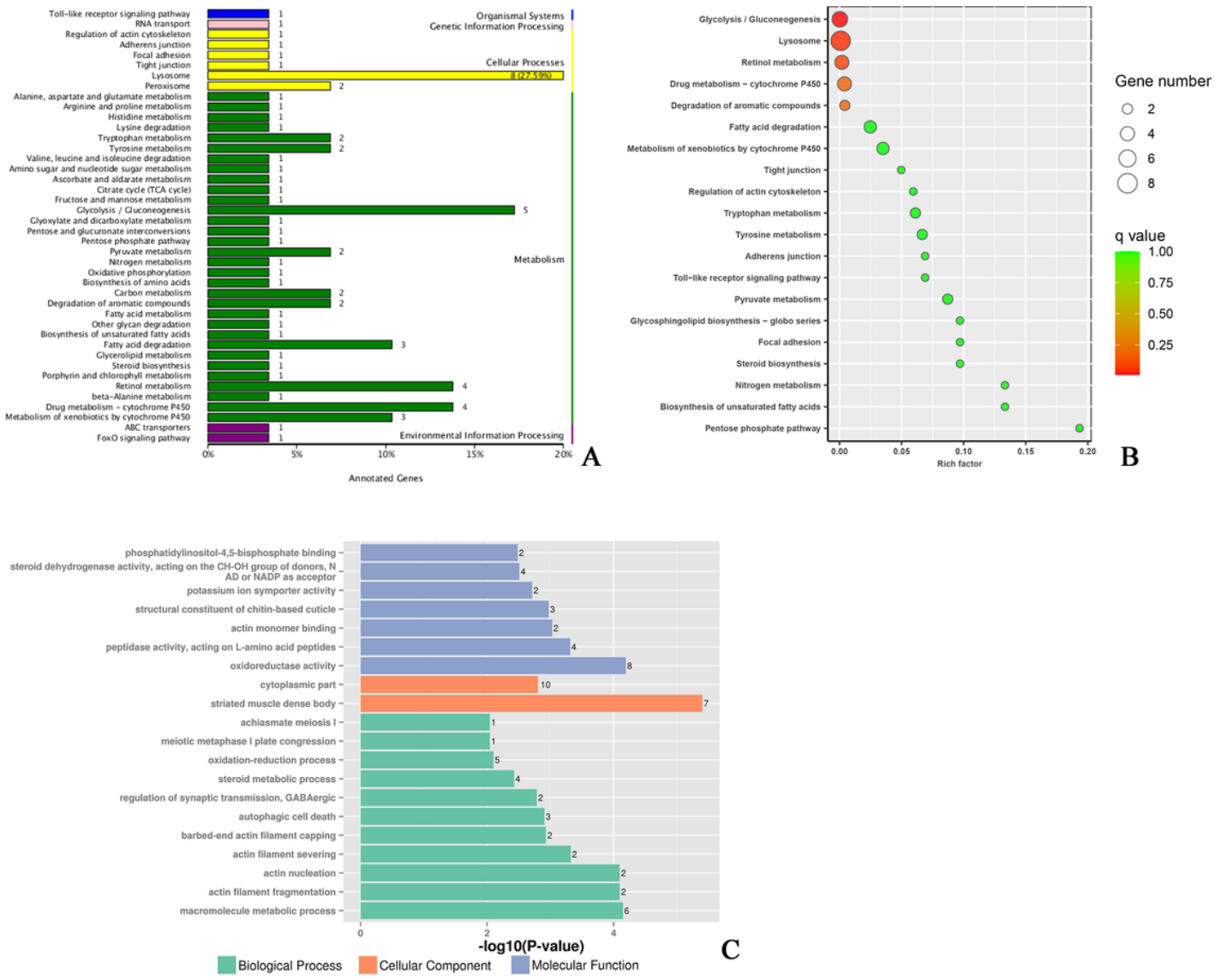

Figure 5

Profiles 6 analysis. (A) KEGG classification of DEGs. (B) Top 20 KEGG pathway enrichment. “q Value” was the value to define the significance of enriched pathways, and its colors represent the significance from green (low) to red (high). The size of the circle represents the number of genes. (C) Top 20 GO enrichment.

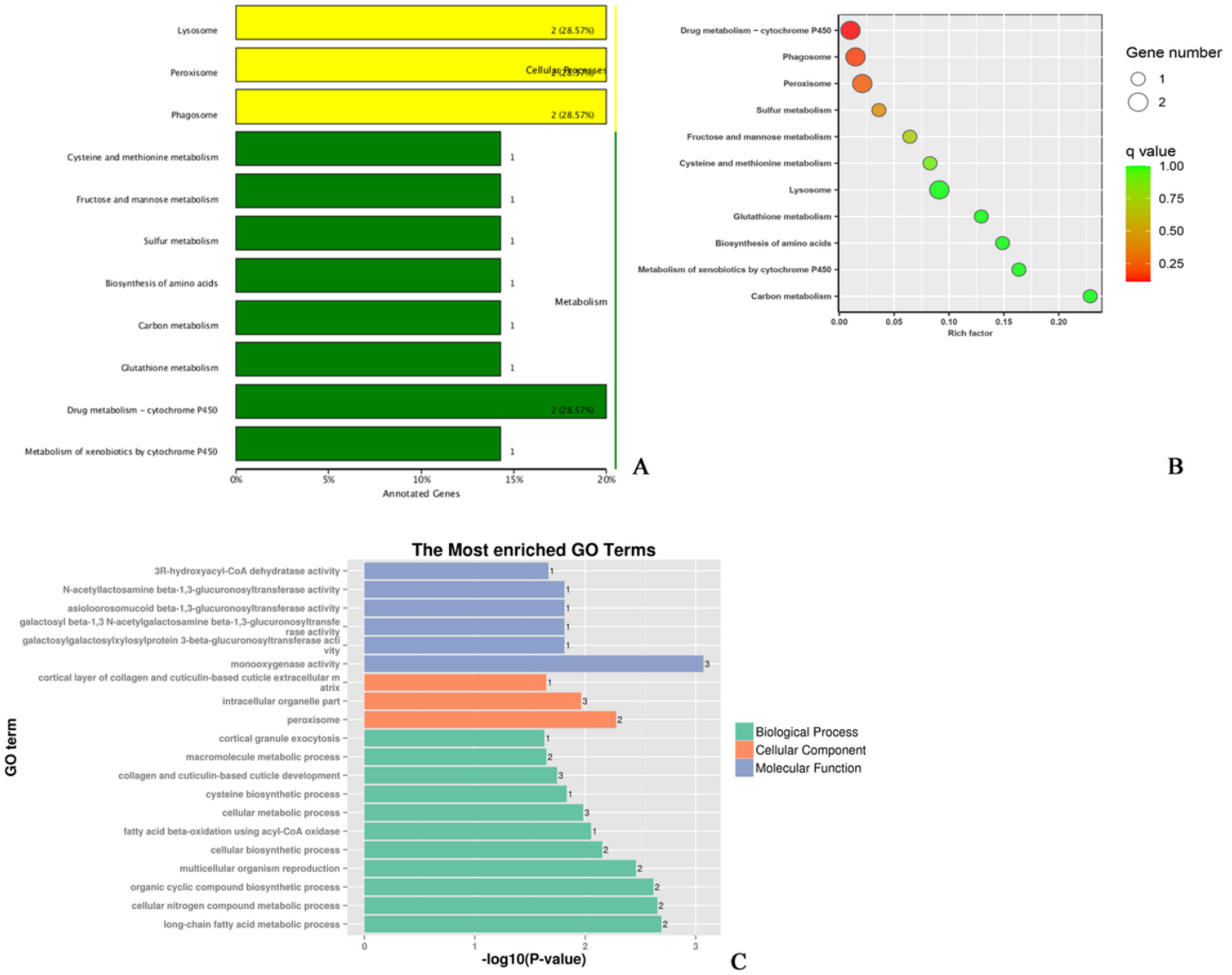

Figure 6

Profiles 7 analysis. (A) KEGG classification of DEGs. (B) Top 20 KEGG pathway enrichment. “q Value” was the value to define the significance of enriched pathways, and its colors represent the significance from green (low) to red (high). The size of the circle represents the number of genes. (C) Top 20 GO enrichment.

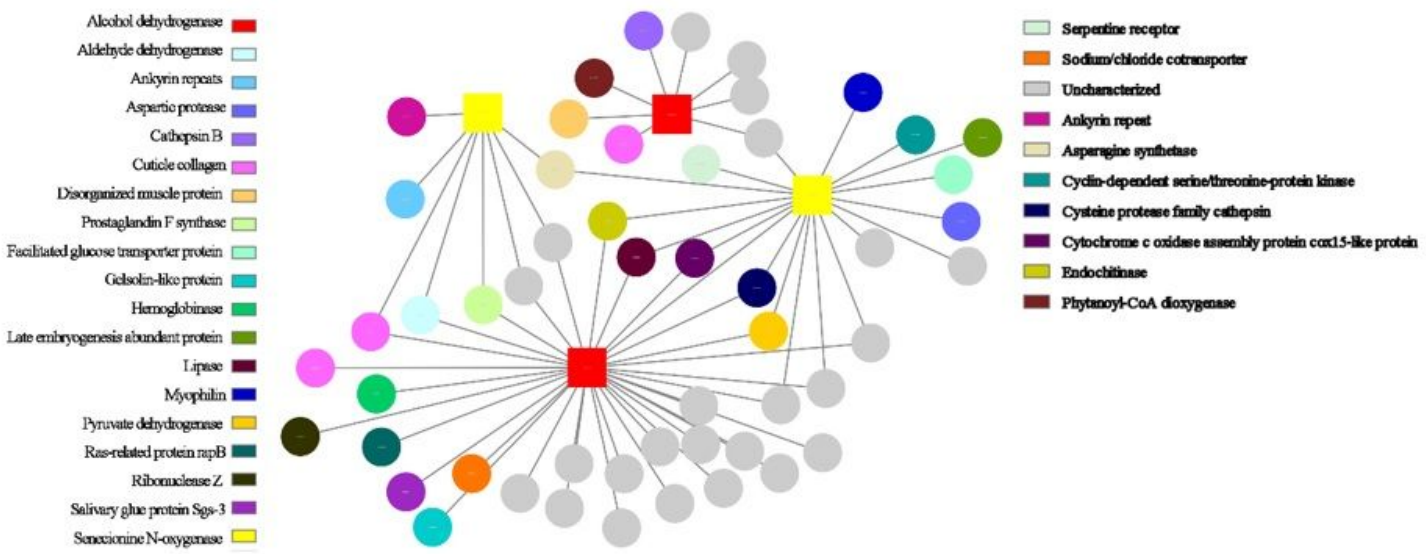

Figure 7

Interaction of gene co-expression patterns in profiles 6, those were used for the construction of the network in Cytoscape 3.7.1. Note: Different colors represent different kinds of genes

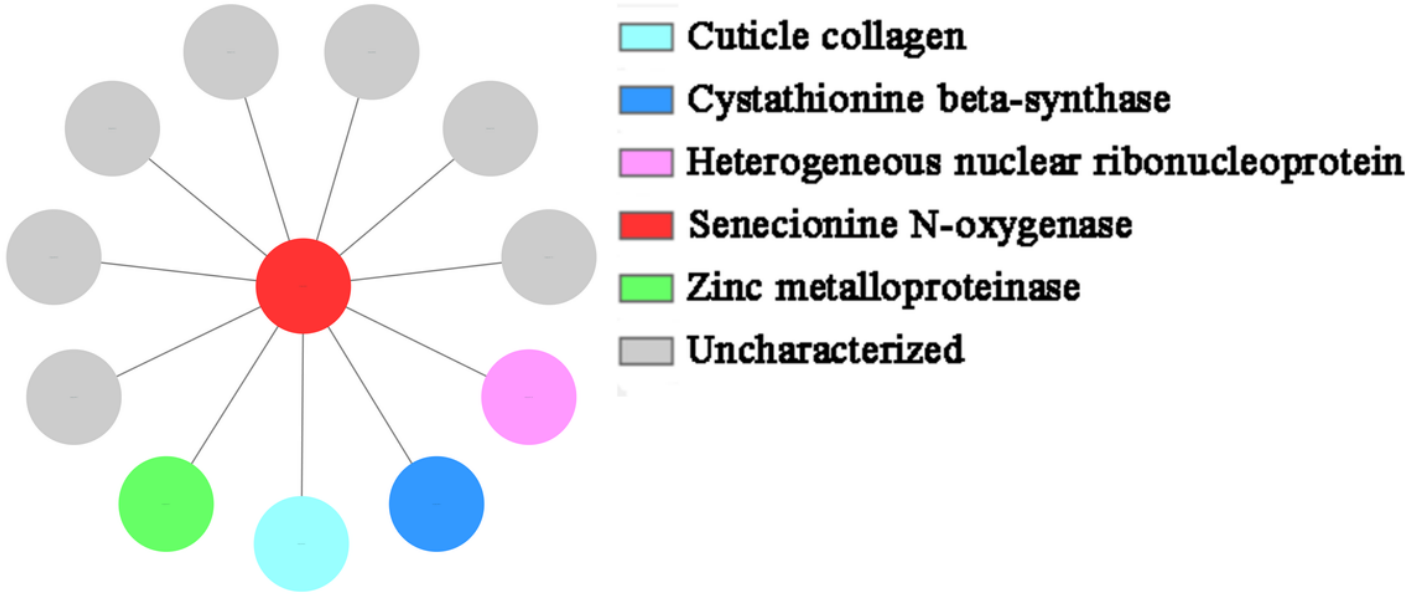

Figure 8

Interaction of gene co-expression patterns in profiles 7, those were used for the construction of the network in Cytoscape 3.7.1. Note: Different colors represent different kinds of genes.

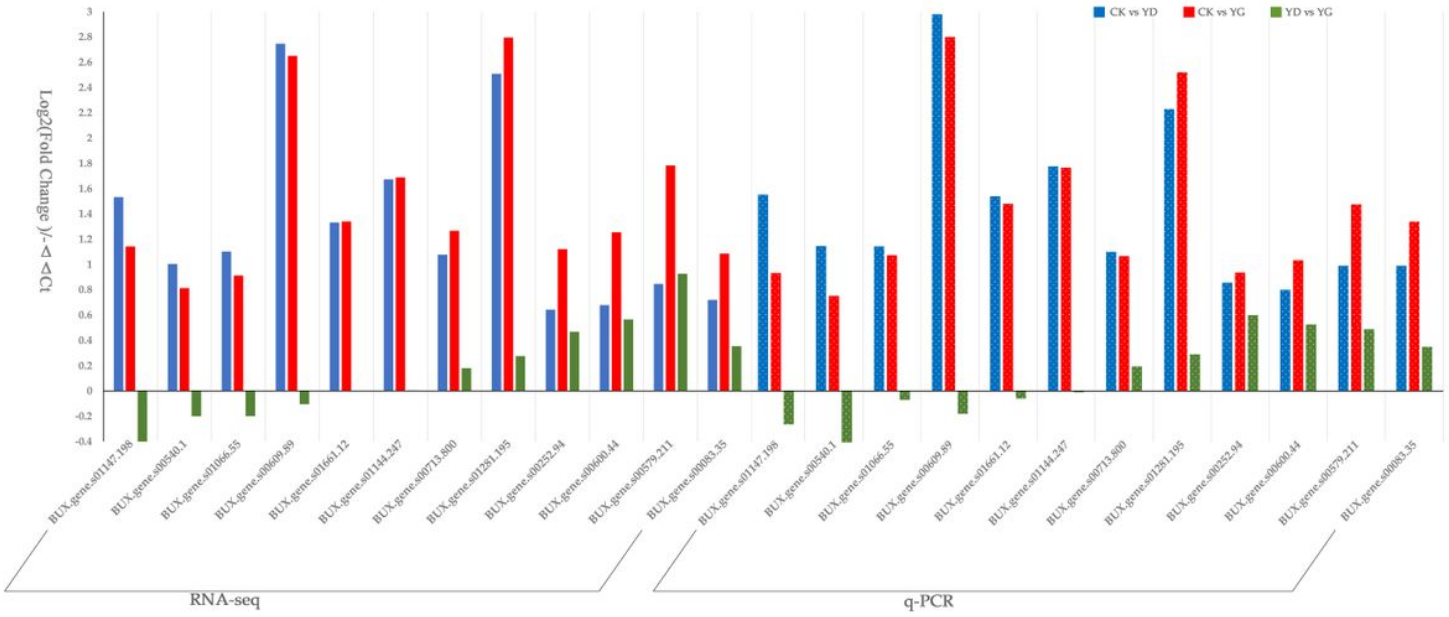

Figure 9

Quantitative real-time polymerase chain reaction (qRT-PCR) of DEGs.

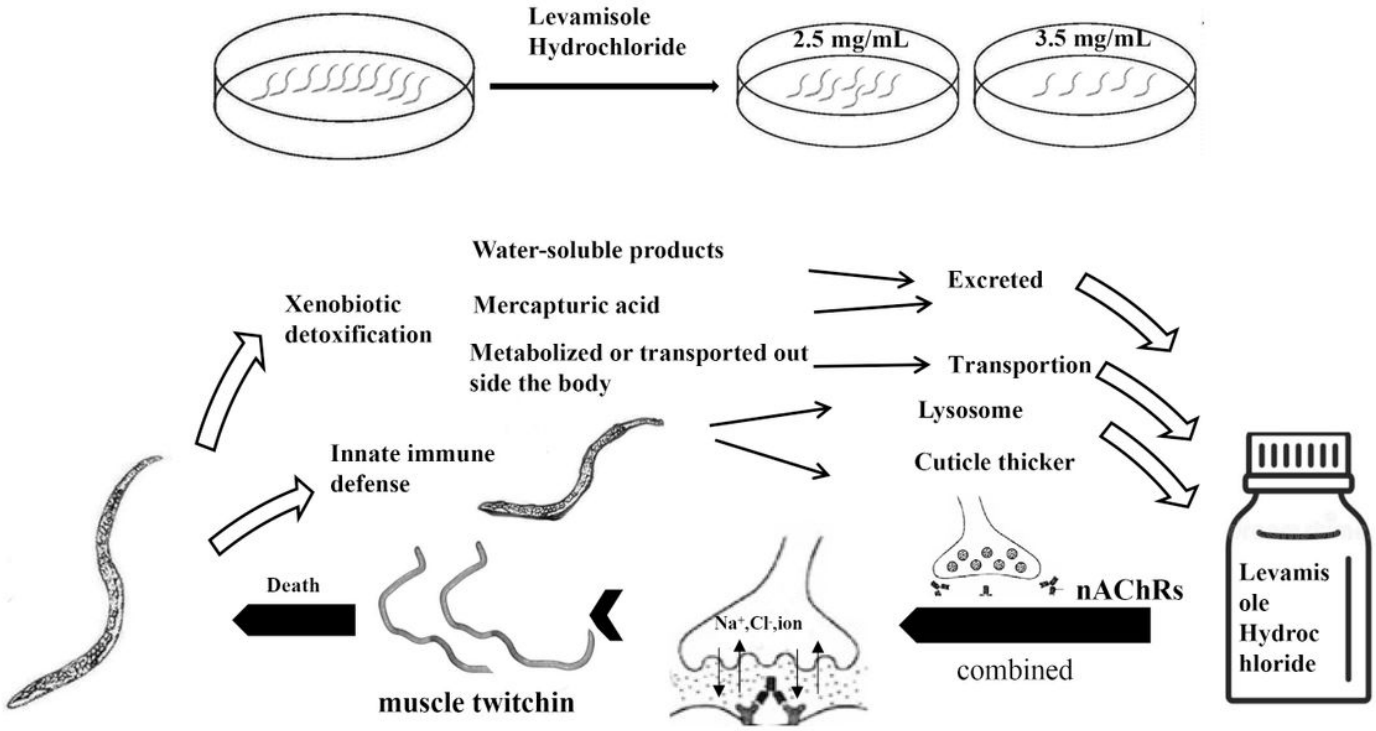

Figure 10

The hypothesis effects of LH on B. xylophilus.

Supplementary Files

This is a list of supplementary files associated with this preprint. Click to download.

- Additionalfile1.xlsx
- Additionalfile2.xlsx
- Additionalfile3.GOClassifiyofDEGsnumbers.xlsx
- Additionalfile4.xlsx
- Additionalfile5.xlsx
- Additionalfile6.xlsx
- Additionalfile7.xlsx
- Additionalfile8.xlsx
- Additionalfile9.Primersusedinpresentstudy.xlsx
- Additionalfile10.png